Proceedings of the 14th International Symposium Ultrafast Phenomena in Semiconductors, Vilnius 2010

THz Emission Induced by an Optical Beating in Nanometer-Length High-Electron-Mobility Transistors

P. Nouvel, J. Torres*, H. Marinchio, T. Laurent, C. Palermo, L. Varani
Institut d'Electronique du Sud-UMR 5214, Montpellier, France

F. Teppe
Groupe d'Etude des Semiconducteurs-UMR 5650, Montpellier, France

P. Shiktorov, E. Starikov, and V. Gruzinskis
Semiconductor Physics Institute, A. Gostauto 11, Vilnius, Lithuania

Experimental results of direct measurement of resonant terahertz emission optically excited in InGaAs HEMT channels are presented. The emission was attributed to two-dimensional plasma waves excited by photogeneration of electron–hole pairs in the HEMT channel at the frequency of the beating of two cw-laser sources. The presence of resonances for the radiation emission in the range of $f_0 \pm 10$ GHz (with f_0 from 0.3 up to 0.5 THz) detected by a Si-bolometer is found. The intensity of THz emission exhibits a nonlinear growth with increase of the pumping power.

PACS: 72.15.Nj, 72.20.Ht, 72.30.+q

1. Introduction

Actually a great advance in the realization of solid-state terahertz (THz) sources comes from the emission of THz radiation from nanometric size electronic structures such as high electron mobility transistors (HEMTs). This is related to three main features of such transistors:

(i) high mobility of carriers in the transistor channel,

(ii) strong nonlinearity of current flowing along the channel governed by a gate,

(iii) possibility of tuning the frequency of 2D plasma waves excited in the channel under the gate by varying the gate potential [1–5].

These peculiarities of carrier transport in the channel allow us to use such transistors both for detection and generation of THz radiation [4, 6]. Recently, the possibility of both resonant and non-resonant detection of THz radiation based on these transistors was verified experimentally (see, e.g. [4] and references therein). However, the other possibility, that is to use them as sources of such a radiation due to spontaneous excitation of plasma waves in the transistor channel (for example, owing to the Dyakonov–Shur instability [1]), up to now is still under investigation [7].

In the present communication the results of direct measurements of emission of THz radiation caused by photoexcitation of 2D plasma waves in InGaAs HEMT channels are presented for the first time.

2. Experimental configuration

The used experimental setup (see Fig. 1) repeats essentially that described in detail in Ref. [8]. Additionally, the new setup includes: (i) the system of THz emission detection, and (ii) the sample cooling system. The THz field emitted by the samples is collected by a 2 inches off-axis-parabolic mirror and focused inside a 4 K Si-bolometer placed close to the mirror. The temperature is decreased by connecting the sample substrate with thermal transfer ribbons immersed into a nitrogen bath. The temperature of the sample is controlled using a thermocouple. To avoid the formation of ice on the HEMT-top-facet, the experiment is made under a helium flow.

Experiments were performed on two HEMTs from InP technology with gate-length values $L_g = 50$ nm and 400 nm. More detailed description of HEMT layers can be found in Ref. [8].

3. Results

The main experimental results are presented in Figs. 2 to 4 which indicate three specific features of the considered phenomena.

* corresponding author; e-mail: jeremi.torres@ies.univ-montp2.fr

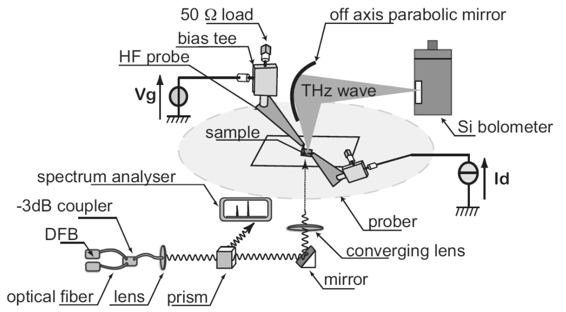

Fig. 1. Experimental configuration scheme. See text for details.

3.1. Static source-to-drain current–voltage

Static source-to-drain current–voltage characteristics of two HEMT structures, namely: for (a) a 50 nm gate length HEMT with a threshold voltage $U_{\mathrm{th}} \approx -350$ mV and for (b) a 400 nm gate length HEMT with $U_{\mathrm{th}} \approx -400$ mV are presented in Fig. 2, (a) and (b), respectively, for a gate potential U_{g} varied in the region of about -300 mV to 0 mV with 100 mV step. Solid and dotted lines correspond, respectively, to 300 K and 200 K lattice temperature. Both HEMTs exhibit the typical current–voltage relation behavior $J_{\mathrm{sd}}(U_{\mathrm{sd}}, U_{\mathrm{g}})$ of source-to-drain current governed by source-to-drain and gate potentials. With decrease of the lattice temperature from 300 to 200 K, an increase of J_{sd} up to 10–15% takes place reaching a maximum value at $U_{\mathrm{g}} \to 0$ V. Such an increase of $J_{\mathrm{sd}}(U_{\mathrm{sd}}, U_{\mathrm{g}})$ agrees well with the change of free-carrier mobility in the HEMT channel. Estimations of the mobility change based on I–V relation at low values of U_{sd} and $U_{\mathrm{g}} \approx 0$ V give about a 20–30% increase in going from 300 K to 200 K. Note that these I–V relations are independent of the operation regime of the source-to-drain circuit, when: (i) either the voltage-driven operation governed by variations of U_{sd}, or (ii) the current-driven operation governed by the current J_{sd} fixed in external circuit are used.

3.2. Radiation emission from HEMT

Radiation emission from HEMT is a signal detected by bolometer. In the absence of an external excitation the experiment does not show any manifestations of radiation emission from HEMTs related to the self-excitation of plasma waves as predicted in Ref. [1]. A sharp resonant growth of the bolometer response was observed only under stimulated photoexcitation at $T = 200$ K (Fig. 3). In this case, the beating frequency was close (with accuracy of ± 10 GHz) to the frequency of the first harmonic of excited plasma waves in the HEMT channel. For the HEMTs with $L_{\mathrm{g}} = 50$ and 400 nm the resonant frequencies are, respectively, $f_0 = 455$ and $f_0 = 325$ GHz (see Ref. [8] for a more detailed explanation) and they are illustrated by Fig. 3a and b, respectively. As follows from Fig. 3 there takes place a sharp resonant emission of radiation in the frequency range $f_0 \pm 10$ GHz. It should be

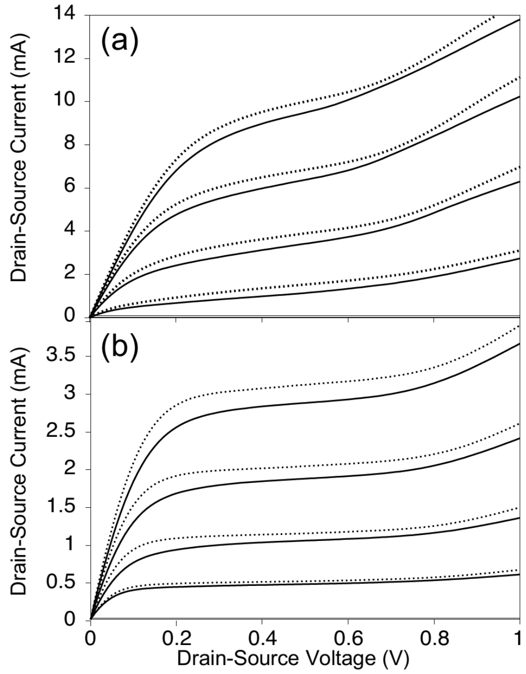

Fig. 2. Output characteristics at 300 K (solid lines) and at 200 K (dotted lines) for a (a) 50 nm and (b) 400 nm gate-length transistor. See text for details.

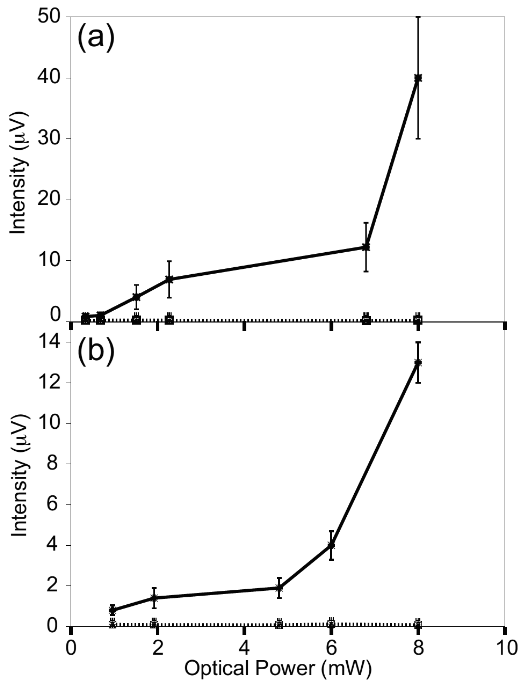

Fig. 3. Beam intensity emitted by the HEMTs and measured by a Si-bolometer at 200 K on the top of HEMT of (a) $L_{\mathrm{g}} = 50$ nm and (b) $L_{\mathrm{g}} = 400$ nm. Solid lines: $f = f_0$ and dotted lines: $f = f_0 \pm 10$ GHz.

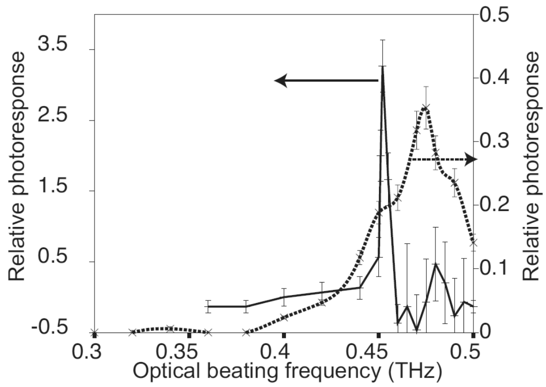

Fig. 4. Measured photoresponse versus the optical beating frequency for 50 nm gate length HEMT ($U_g = -0.2$ V, $I_{sd} = 4$ mA at $T = 300$ K (dotted line) and at 200 K (solid line). Error-bars are experimental data joined by eye guidelines.

stressed that the bolometer response dependence on the pumping power is non-linear. With the increase of the beating frequency deviation from the resonant frequencies f_0 more than 10 GHz, the bolometer response signal went back to the thermal noise level. The minimum frequency step of 10 GHz is dictated by the frequency resolution realized in the beating experiments. The resonant emission takes place under the saturation of static I–V curves only (see Fig. 2a and b), that is at $U_{sd} \geq 0.2$ V. For smaller values of U_{sd}, the bolometer response remained within the thermal noise.

3.3. Rectification of induced ac currents in HEMT channel

Due to the nonlinear character of the current flow in HEMT channels there exists a possibility to realize a self--control of the induced plasma wave intensity by measuring, under fixed drain current regime, the dc component of the source–drain voltage drop U_{sd} as a function of the external signal frequency f. Figure 4 illustrates the dependence of the relative magnitude of such a photoresponse R_f for the HEMT with $L_g = 50$ nm

$$R_f = \frac{U_{sd}(f) - \overline{U_{sd}}}{\overline{U_{sd}}}, \qquad (1)$$

where $U_{sd}(f)$ is the source–drain voltage at the beating frequency f, while $\overline{U_{sd}}$ is the source–drain voltage drop at $f = 0$. Here solid and dotted lines correspond to measurements performed at 300 and 200 K, respectively and were obtained for the maximum pumping power of 8 mW provided by the laser system. As follows from Fig. 4, the self-detection has a resonant character with a peak at frequencies $f_0 = 475$ and 455 GHz at 300 and 200 K, respectively. Let us note that at $T = 200$ K the resonant frequency of self-detection coincides exactly with the resonant frequency obtained in measurements of the emission intensity (see Fig. 3). As one can see from Fig. 4, the resonance linewidth described by the full width at half maximum (FWHM) sharply decreases from 40 to 5 GHz with temperature decrease from 300 to 200 K. Let us note that the estimation of the FWHM at $T = 200$ K corresponds to the limiting value determined by the accuracy of the measured beating frequency. Therefore, the FWHM real value can be even less than the above estimation. An important difference in the results of emission and self-detection is that at 300 K the bolometer does not detect any emission of radiation while the self-detection indicates a resonant photoexcitation of plasma waves at a slightly blue-shifted frequency $f_0 = 475$ GHz (with respect to 455 GHz).

Summarizing experimental results we can state that in going from 300 to 200 K:

(i) the static I–V relations are slightly changed showing about 20–30% variation of a carrier-mobility in the HEMT channel,

(ii) both techniques (based on emission and rectification spectra) allow us to detect photoexcited plasma waves in the HEMT channel with dispersion of 2D plasma waves predicted by the analytical approach [9],

(iii) the direct radiation emission was measured only at 200 K while at 300 K it was absent,

(iv) the detection by using rectification effects shows a photoexcitation of plasma waves at both 300 and 200 K with a resonance quality increase of about one order of magnitude.

As a consequence one can conclude that the observed resonant emission at $T = 200$ K is directly related to the induced excitation of 2D plasma waves, since: (i) the emission is absent with the absence of photoexcitation, and, (ii) the resonant frequency values coincide with those predicted by the analytical theory [9].

4. Conclusion

Let us consider possible interpretations of the obtained results. The experimentally observed shrinking of the resonance linewidth by one order of magnitude while the increase of the carrier mobility is up to 20–30% only, allows us to suppose that, in going from 300 to 200 K, the plasma-wave instability threshold (see, e.g., [1]) is approached or slightly surpassed. In these conditions the emission results can be interpreted in two ways. On the one hand, supposing that the sensitivity of the whole system (mirrors and bolometer) used for THz emission detection is insufficient to detect excitation of weak self--oscillations, we measure merely an induced resonant emission at a high-level of photoexcitation. However, in this case the detected emission power must be linearly related to the optical pumping power. On the other hand, one can suppose that there takes place a hard start-up of self-oscillations which occur in nonlinear systems under a certain finite amplitude of an external action. The latter regime allows us to explain the sharp nonlinear growth of the radiation emission intensity with increase of the photoexcitation power. In both cases, further more detailed experiments are required to clarify these explanations.

Acknowledgments

Authors wish to thank T. Gonzalez, J. Mateos (University of Salamanca, Spain) for useful discussions; S. Bollaert and Y. Rollens (IEMN-UMR 5820) for providing the samples and GIS "TeraLab". This work was partially supported by grant No. MIP-10278 of Lithuanian Science Council.

References

[1] M. Dyakonov, M. Shur, *Phys. Rev. Lett.* **71**, 2465 (1993).

[2] A.P. Dmitriev, A.S. Furman, V.Y. Kachorovskii, *Phys. Rev. B* **54**, 14020 (1996).

[3] A.P. Dmitriev, A.S. Furman, V.Y. Kachorovskii, G.G. Samsonidze, G.G. Samsonidze, *Phys. Rev. B* **55**, 10319 (1997).

[4] W. Knap, J. Lusakowski, T. Parenty, S. Bollaert, A. Cappy, V.V. Popov, M.S. Shur, *Appl. Phys. Lett.* **84**, 2331 (2004).

[5] F. Teppe, W. Knap, D. Veksler, M. Shur, A.P. Dmitriev, V.Y. Kachorovskii, S. Rumyantsev, *Appl. Phys. Lett.* **87**, 052107 (2005).

[6] D. Veksler, F. Teppe, A.P. Dmitriev, V.Y. Kachorovskii, W. Knap, M.S. Shur, *Phys. Rev. B* **73**, 125328 (2006).

[7] N. Dyakonova, A.E. Fatimy, J. Lusakowski, W. Knap, M.I. Dyakonov, M.-A. Poisson, E. Morvan, S. Bollaert, A. Shchepetov, Y. Roelens, C. Gaquiere, D. Theron, A. Cappy, *Appl. Phys. Lett.* **88**, 141906 (2006).

[8] P. Nouvel, H. Marinchio, J. Torres, C. Palermo, L. Chusseau, D. Gasquet, L. Varani, P. Shiktorov, E. Starikov, V. Gružinskis, *J. Appl. Phys.* **106**, 013717 (2009).

[9] H. Marinchio, G. Sabatini, J. Pousset, C. Palermo, J. Torres, L. Chusseau, L. Varani, E. Starikov, P. Shiktorov, *Appl. Phys. Lett.* **94**, 192109 (2009).